

GradNet: A Gradient-Based Framework for Optimal Network Science

Guram Mikaberidze
School of Computing
University of Wyoming
Email: gmikaber@uwoyo.edu

Beso Mikaberidze
Muskhelishvili Institute of
Computational Mathematics
Georgian Technical University

Dane Taylor
School of Computing
Department of Mathematics & Statistics
University of Wyoming

Abstract—Network science has traditionally examined how structure determines dynamics. Here we invert this paradigm: we ask how functional dynamics and resource constraints shape network architecture. We introduce GradNet, an AI-enabled optimization framework that treats network topology as a continuously differentiable object. This allows designing networks that optimize arbitrary dynamical objectives—from synchronization to communication capacity—under realistic constraints. Applying this framework across diverse systems reveals that canonical network features emerge spontaneously from constrained optimization rather than requiring explicit imposition. Optimizing Kuramoto oscillator synchronization under fixed coupling budgets produces sparse, bipartite, frequency-disassortative architectures that eliminate classical synchronization thresholds. Minimizing social tension in opinion dynamics reproduces the empirically observed factional split in Zachary’s karate club network. Maximizing entanglement distribution in spatial quantum networks under distance-dependent costs recovers minimum spanning tree architectures. These results demonstrate that optimization acts as both an engineering tool for network design, scalable to networks exceeding 10^5 nodes, and a scientific probe revealing fundamental structure-function relationships. By recasting network architecture as the solution to constrained optimization problems, this variational perspective offers a unified framework connecting network analysis, design, and inference across physical, biological, and technological systems.

I. INTRODUCTION

Networks pervade the natural and engineered world, and network science has largely focused on how structure shapes dynamics. Here we invert the lens: functional demands and constraints shape structure through optimization. From power grids and transportation systems to neural circuits and ecological webs, complex systems are often described as dynamical processes unfolding over an underlying network of interactions [1], [2]. Over the past two decades, network science has revealed how structural properties, such as degree heterogeneity, modularity, small-world organization, and sparsity, shape collective behavior [3], [4], [5], [6], [7]. In many studies, network structure is treated as fixed or sampled from a prescribed generative family, such as Erdős–Rényi or Watts–Strogatz models [8], [9]. One then analyzes dynamics on that topology. Here we emphasize the complementary paradigm: optimizing topology itself to support desired dynamics or performance objectives [10], [11], [12], [13].

In many real-world systems, this separation is artificial. In these settings, structure is a decision variable. Biological

networks are shaped by evolutionary pressures; infrastructure networks are redesigned under economic and physical constraints; communication systems are engineered to optimize performance under resource limitations. In such settings, structure is not a static backdrop for dynamics but an adaptive object shaped by functional demands. This raises a fundamental question: can network structure itself be understood as the outcome of principled optimization? Variants of this question have appeared repeatedly in discussions of complex networks [14], [15], [16], yet systematic computational frameworks capable of addressing it across dynamical objectives and structural constraints remain limited. We explore the idea that constrained optimization can act as a generative mechanism for network architecture.

Optimization principles have long provided unifying explanations across scientific disciplines [15], see Table I. These principles not only explain outcomes; they also provide predictive or constructive tools for inference and fundamental understanding. The principle of least action in physics, loss minimization in machine learning, utility maximization in economics, and fitness maximization in evolutionary biology all recast complex phenomena as solutions to variational problems. In contrast, despite the centrality of networks in modern science, systematic optimization-based formulations of network structure remain

Field	Variational / Optimization Principle
Physics	Principle of least action
Machine learning	Loss minimization
Evolutionary biology	Fitness maximization
Economics	Utility maximization
Information theory	Rate–distortion optimization
Statistics	Maximum likelihood estimation
Control theory	Optimal control
Network science	Optimal network design (emerging)

TABLE I: Many scientific disciplines admit formulations in terms of variational or optimization principles, which provide unifying, explanatory frameworks complementary to dynamical, empirical, statistical, and mechanistic approaches. Shown are representative examples across fields. In network science, despite a wealth of empirical and theoretical results, systematic optimization-based formulations remain comparatively underdeveloped and fragmented. This motivates the emerging view of optimal network design, for which this work provides a general numerical framework.

comparatively fragmented across disparate objective classes and constraint types. While numerous studies investigate how dynamics behave on given networks—or across parameterized families of networks with built-in structural properties—far fewer treat network topology and weights themselves as variables to be optimized under explicit constraints.

We argue that constrained optimization constitutes a powerful and under-explored mechanism of network emergence, complementing common accounts based on growth rules, local heuristics, or generative ensembles [14], [16]. Rather than prescribing structural features a priori—either by fixing a specific topology or by sampling from generative ensembles that encode properties such as sparsity or small-world structure—we treat networks as objects that adapt to maximize or minimize well-defined performance objectives under resource, geometric, or physical constraints. In this view, canonical structural properties—such as sparsity, bipartition, modular organization—need not always be assumed as primitives. Instead, they may arise as consequences of constrained resource allocation under budgets, geometry, symmetry, and sign constraints. This perspective shifts the focus of network science from descriptive analysis of observed structures toward constructive principles governing why those structures appear.

Related work has explored optimization of networks for improved robustness [17], [18], [19], [20], [21], [22], [23], stronger synchronizability [24], [25], [26], [27], [28], [29], mitigated epidemic spreading [30], [31], [32], [33], network controllability [34], [35], algebraic connectivity [36], effective resistance [37], and transportation [38]. This research spans varied optimization settings, including directed [24], [35] and weighted [30], [24], [36], [37], [23], [35] networks, as well as the construction of optimal networks from scratch [25], [36]. Other papers optimize networks by adding/removing nodes [31] or fine-tuning node locations [39].

The vast majority of prior research cited above optimizes spectral measures of networks. This class of problems is particularly attractive because many dynamical properties of networks can be expressed in terms of the spectrum [40], [41], [42], [43], [44]. This often allows efficient optimization, since one can compute the network spectrum for each proposed mutation rather than having to simulate the dynamics. Additionally, one can use perturbation theory to approximate the fitness of the proposed mutations even more quickly than full spectral computation [33], [32].

Most existing approaches rely on zeroth-order optimization, gradually rewiring edges to improve performance measures. Common strategies include greedy rewiring [17], [19], [22], [31], [32], [33], [38], simulated annealing [25], [26], [27], and convex optimization formulations [35], [36], [37] when the objective permits it. Others develop methods that are designed for and applicable to their respective tasks [34]. Notable exceptions are the cases when the gradients can be calculated explicitly [28], [30], though these are few and far between. Given that search in most cases is zeroth order, the cited research mostly deals with networks of the order 10^3 – 10^4 nodes.

A recent line of work approaches network optimization from the perspective of Graph Neural Networks [45], [46] where networks are being rewired on the fly to help improve predictive capability of the machine learning model. This line of work is closest to our methodology, but pursues very different objectives.

Despite these advances, existing approaches remain limited in two important ways: most rely on zeroth-order search over discrete rewiring operations, and many are restricted to spectral objectives that avoid simulating network dynamics. A general framework capable of optimizing arbitrary dynamical objectives over large networks remains largely absent.

Recent advances in machine learning offer an opportunity to address this gap. Automatic differentiation [47] and hardware-accelerated optimization have transformed the optimization of high-dimensional models. These tools enable gradients to be computed through complex computational graphs, including the numerical integration of differential equations. We argue that these same tools can be repurposed to optimize network structure itself. By treating the adjacency matrix as a continuously parameterized object constrained to an admissible set via smooth parameterizations, network design problems become amenable to gradient-based optimization under arbitrary differentiable objectives, see Fig. 1.

To operationalize this variational view, we introduce *GradNet*, a general first-order optimization framework for networks [48]. We formulate the space of admissible networks as a smoothly parameterized subset of a high-dimensional space, with resource constraints, symmetry conditions, geometric restrictions, and edge sign constraints encoded directly into this parameterization. A scalar objective function—depending either directly on network structure or indirectly on the outcome of discrete- or continuous-time dynamics unfolding on the network—is then optimized via gradient-based methods. Gradients are computed automatically and efficiently, even when the objective requires repeated numerical integration of dynamical systems. To support such computationally intensive workflows, *GradNet* provides built-in ODE simulation on networks, GPU acceleration, TensorBoard integration for real-time monitoring of optimization progress, and seamless export to *NetworkX* for downstream analysis. With this, *GradNet* is able to optimize networks of up to 10^5 within reasonable times.

Beyond providing a flexible computational tool, this framework reveals a deeper principle: optimality often induces structural regularity. Networks optimized for specific objectives under constraints frequently collapse high-dimensional combinatorial complexity into low-dimensional structure. Critical-point conditions and variational analysis can then yield analytical characterizations of optimal architectures even when analytics is not feasible for arbitrary networks. Thus, computation and theory inform one another: numerical optimization uncovers structural regularities, and optimality conditions render those regularities mathematically tractable.

We demonstrate the breadth of this approach across diverse case studies, spanning design, modification, and inference. Across these examples, we observe that structural features can

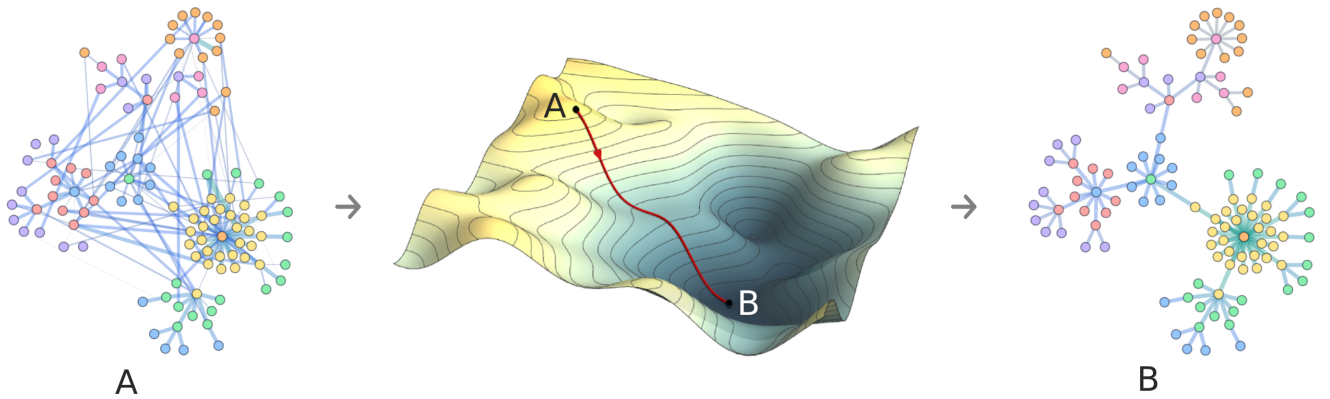


Fig. 1: **Illustration of the optimal network science framework proposed in this paper.** The optimization space consists of all admissible networks satisfying problem-specific constraints, such as directionality, fixed construction budgets, and the non-physicality or impossibility of certain edges. A scalar objective function is defined over this network space to quantify the fitness of a network for the task at hand. Starting from an initial network configuration (A), the network is iteratively modified via gradient-based optimization to minimize this objective function, ultimately yielding an optimal network configuration (B).

emerge spontaneously from constrained optimization rather than being imposed explicitly. In particular, in several of our case studies, sparsity arises as an emergent property, even in the absence of sparsity penalties. We also observe the emergence of bipartition, minimum-spanning-tree-like backbone, and community partitioning when objectives and constraints favor them.

Collectively, these results suggest a reframing of network science: from descriptive analysis of fixed structures toward constructive principles for design and inference under constraints. Instead of viewing structural features as descriptors to be explained by fixed topologies or generative mechanisms alone, we propose treating network architecture as the outcome of principled optimization under constraints. This perspective unifies analysis, design, and inference within a single variational framework and opens new directions for both theoretical and applied research in complex systems.

II. OPTIMIZATION FRAMEWORK

We define the *optimization space* as the set of all *admissible* network structures, where admissibility is determined by application-specific constraints. In general, these constraints encode structural, physical, technical, or policy-related limitations that restrict which network configurations are feasible. The resulting admissible set typically forms a constrained, finite-dimensional subset of a high-dimensional space of network representations.

To make this definition concrete, consider the problem of improving a power-grid network under a fixed budget. In this setting, the network is geometric and undirected. Although some absent connections may be added in principle, others are disallowed due to physical geography, engineering limitations, or logistic and political considerations. As a result, the optimization is carried out over the space of symmetric adjacency matrices A_{ij} with non-negative entries that represent

power-line conductances. Self-loops are excluded, implying $A_{ii} = 0$, and additional constraints may fix certain off-diagonal entries to zero, further reducing the dimensionality of the feasible space.

The optimization process begins from an initial network configuration A_{ij}^0 and is subject to a total budget b . Accordingly, the admissible set can be viewed as a neighborhood centered at A_{ij}^0 with radius b in the space of network configurations. Distances within this space are measured using a weighted ℓ_1 norm (i.e., the Manhattan distance), which reflects the assumption that the total modification cost is the sum of the individual expenditures associated with changing each edge. Heterogeneity in construction or upgrade costs is incorporated through a cost matrix C_{ij} , which assigns a weight to each dimension of the optimization space.

More generally, the framework accommodates a wide range of network design scenarios. Networks may be directed or undirected, constructed from scratch or modified from an existing configuration. Edge weights may be constrained to be nonnegative, nonpositive, or unrestricted, and admissible modifications may similarly be limited to edge weight increases, decreases, or both. Resource constraints need not be restricted to an ℓ_1 budget; instead, they may be expressed using an arbitrary ℓ_p norm, allowing the modeling of diverse cost structures and trade-offs.

Networks are optimized with respect to a scalar objective, known as a loss function, which quantifies network performance. In the power-grid example, such objectives might include minimizing construction cost (e.g., total material usage), limiting operational risk (e.g., the maximum power-line temperature), or optimizing other performance or resilience metrics. Importantly, the loss function may depend either directly on the network topology or indirectly on the outcome of a dynamical process unfolding on the network. In both cases, optimization is performed via gradient-based methods

over the admissible network space to identify configurations that minimize the chosen loss. Gradients are computed using automated differentiation which can seamlessly handle even lengthy numerical integration of dynamical processes unfolding on the network.

For each configuration of network constraints and symmetries, we introduce a smooth parameterization of the bounded space of admissible networks via unconstrained parameters $\mathbf{P} \in \mathbb{R}^K$. These parameterizations provide continuous and exhaustive representations of their respective admissible sets, enabling gradient-based optimization to traverse the space freely while remaining strictly within its prescribed bounds. All this is possible within the *GradNet* python package [48].

III. ALGORITHM

Let us describe how the adjacency matrix $\mathbf{A} \in \mathbb{R}^{N \times N}$ is constructed from a set of trainable parameters $\mathbf{P} \in \mathbb{R}^{N \times N}$ across a range of network design scenarios. The key idea is to treat \mathbf{P} as an unconstrained parameter matrix and map it, through a sequence of differentiable transformations, into a well-formed adjacency matrix that satisfies all structural, sign, and resource constraints. This encoding defines a smooth map $\mathbf{A} = g(\mathbf{P})$, enabling gradient-based optimization over admissible networks. Later, we discuss how this parameterization can be reduced to far fewer than N^2 degrees of freedom when the network is known *a priori* to be sparse.

The framework accommodates a broad class of design problems. Networks may be directed or undirected, built from scratch or obtained via modifications to an existing configuration. Edge weights may be constrained to be nonnegative, nonpositive, or unrestricted, and permissible updates may likewise be restricted to increases, decreases, or both. Resource constraints are not limited to an ℓ_1 budget; more generally, expenditures can be aggregated using an arbitrary ℓ_p norm, allowing heterogeneous cost structures and nonlinear trade-offs to be modeled. All of these design choices are incorporated systematically through the encoding pipeline described below.

Step 1: Directed/undirected networks. In many applications, the network is fundamentally undirected, and therefore its adjacency matrix must be symmetric. We enforce this structural constraint by symmetrizing the parameter matrix:

$$\mathbf{S} = \begin{cases} \mathbf{P}, & \text{if the network is directed,} \\ \frac{1}{2}(\mathbf{P} + \mathbf{P}^\top), & \text{if the network is undirected.} \end{cases}$$

Step 2: Modification sign constraints. Depending on whether edge weights are allowed to increase (e.g., build or reinforce), decrease (e.g., demolish or weaken), or change in either direction, we impose sign constraints on the modifications:

$$T_{ij} = \begin{cases} S_{ij}, & \text{if arbitrary changes are allowed,} \\ S_{ij}^2, & \text{if only nonnegative changes are allowed,} \\ -S_{ij}^2, & \text{if only nonpositive changes are allowed.} \end{cases}$$

Step 3: Edge masking. Certain edges may be infeasible to construct or modify due to physical, geometric, or policy constraints. These restrictions are encoded in a mask matrix \mathbf{M} , where $M_{ij} = 1$ if the edge (i, j) is allowed and $M_{ij} = 0$ otherwise.

If no mask is provided, we assume that all edges except self-loops are admissible and initialize

$$M_{ij} = 1 - \delta_{ij},$$

where δ_{ij} denotes the Kronecker delta.

We then eliminate forbidden modifications via elementwise multiplication:

$$\mathbf{U} = \mathbf{T} \odot \mathbf{M}.$$

This operation sets all disallowed edge modifications to zero while retaining the admissible ones.

Step 4: Budget constraint. We now constrain the magnitude of the modification to satisfy the allocated budget b . The budget is enforced using a cost matrix \mathbf{C} together with an aggregation norm p . The parameter p determines the elementwise ℓ_p norm used to aggregate costs across edges (for example, $p = 2$ corresponds to the Frobenius norm). The entry C_{ij} represents the cost of changing the edge weight between nodes (i, j) by one unit. These costs may vary across node pairs—for example, they may be proportional to geometric distance.

If no cost matrix is provided, we assume uniform costs and set $C_{ij} = 1$ for all admissible edges. The default aggregation norm is $p = 1$, corresponding to a simple sum of costs per edge.

We first compute the scaling factor

$$\gamma = \frac{b}{\|\mathbf{C} \odot \mathbf{U}\|_p}.$$

This scalar rescales the proposed modification so that the total cost matches (or respects) the prescribed budget. Depending on the problem formulation, the budget may be enforced exactly, imposed as an upper bound, or omitted entirely:

$$\Delta = \begin{cases} \gamma \mathbf{U}, & \text{if } b \text{ is enforced exactly,} \\ \min(\gamma, 1) \mathbf{U}, & \text{if } b \text{ is an upper bound,} \\ \mathbf{U}, & \text{if there is no budget constraint.} \end{cases}$$

Step 5: Forming the adjacency matrix. With Δ determined, we construct the updated adjacency matrix as

$$\tilde{\mathbf{A}} = \mathbf{A}^{(0)} + \Delta.$$

Here $\mathbf{A}^{(0)}$ denotes the initial adjacency matrix prior to optimization. If an initial network is provided, Δ represents modifications to that baseline structure. If no initial network is specified, we set

$$\mathbf{A}^{(0)} = 0,$$

which corresponds to constructing the network entirely from scratch.

Case study	Directed or undirected	Modification signs	Mask	Resource constraint form	Modify or build	Edge-weight signs	Objective type
Logical gates	Directed	Unconstrained	N/A	N/A	Build	Unconstrained	Dynamic (discrete)
Algebraic connectivity	Undirected	Nonnegative	2D grid	$b = \frac{1}{N} \sum_{ij} A_{ij}$	Build	Nonnegative	Static
Kuramoto synchrony	Undirected	Nonnegative	N/A	$b = \frac{1}{N} \sum_{ij} A_{ij}$	Build	Nonnegative	Dynamic (continuous)
Zachary’s Karate Club	Undirected	Nonpositive	N/A	N/A	Modify	Nonnegative	Dynamic (continuous)
Network reconstruction	Undirected	Nonnegative	N/A	$b = \frac{1}{N} \sum_{ij} A_{ij}$	Build	Nonnegative	Dynamic (continuous)
Quantum internet	Undirected	Nonnegative	N/A	$b = \frac{1}{N} \sum_{ij} C_{ij} A_{ij}$	Build	Nonnegative	Static

TABLE II: **Summary of the case studies and their optimization setups.** For each problem, we report the properties as outlined in the Algorithms section: (i) network type (undirected $\mathbf{A} = \mathbf{A}^T$, or directed); (ii) sign constraints on permissible updates ($\Delta_{ij} \geq 0$, $\Delta_{ij} \leq 0$, or unconstrained); (iii) the feasibility mask \mathbf{M} constraining admissible edge additions/modifications; (iv) the presence and type of the budget constraint b ; (v) whether *GradNet* learns the network from scratch ($\mathbf{A}^{(0)} = 0$) or optimizes a given initial network $\mathbf{A}^{(0)}$; (vi) sign constraints on edge weights ($A_{ij} \geq 0$, $A_{ij} \leq 0$, or unconstrained); and (vii) the objective/loss \mathcal{L} , classified as static (structure-only) or dynamics-dependent (arising from a discrete- or continuous-time process on the network). In most cases budgets are either unconstrained or have fixed ℓ_1 norm; the last case has different costs for each edge because the network is geometric and edge construction between the nodes (i, j) is proportional to the distance between them C_{ij} .

Step 6: Edge weight sign constraints. Finally, we enforce the prescribed sign constraints on the edge weights to obtain the final adjacency matrix:

$$\mathbf{A} = \begin{cases} \tilde{\mathbf{A}}, & \text{if edge weights are unconstrained,} \\ |\tilde{\mathbf{A}}|_\epsilon, & \text{if edge weights must be nonnegative,} \\ -|\tilde{\mathbf{A}}|_\epsilon, & \text{if edge weights must be nonpositive.} \end{cases}$$

Here $|\cdot|_\epsilon$ denotes a smooth approximation of the absolute value, introduced to avoid non-differentiable kinks in the loss landscape. For a scalar x , it is defined as

$$|x|_\epsilon = x \tanh\left(\frac{x}{\epsilon}\right),$$

where $\epsilon \ll 1$ is a small smoothing parameter.

It is important to note that when the sign constraints imposed on the modifications Δ conflict with the sign constraints imposed on the final edge weights \mathbf{A} , the pipeline may not simultaneously satisfy the modification-sign constraint and exact budget exhaustion. In such cases, strict adherence to both conditions cannot be guaranteed. To avoid ambiguity, the *GradNet* package automatically detects and reports any such violations to the user.

If the network is undirected, then $\mathbf{A}^{(0)}$, \mathbf{M} , and \mathbf{C} must be symmetric. This condition is verified and, when necessary, enforced by *GradNet* to ensure consistency of the optimization space.

GradNet supports two encoding modes: dense and sparse. When the network is known *a priori* to be sparse, meaning that most edges are infeasible and the mask matrix \mathbf{M} is largely zero, it is inefficient to store and manipulate matrices in dense form. In such cases, we recommend representing \mathbf{M} using sparse *PyTorch* tensor. The entire encoding pipeline is then

executed in sparse form, requiring $O(E)$ memory, where E denotes the number of admissible edges, instead of $O(N^2)$. This also avoids unnecessary dense matrix operations, resulting in substantial savings in both memory usage and computational cost.

With the pipeline defined above, the trainable parameters \mathbf{P} are mapped to a well-formed adjacency matrix $\mathbf{A} = g(\mathbf{P})$, on which the user-defined loss function $\mathcal{L}(\mathbf{A})$ is evaluated. In the simplest setting, using standard gradient descent, the parameters are updated according to

$$P_{ij}^{(n+1)} = P_{ij}^{(n)} - \eta \frac{\partial \mathcal{L}(\mathbf{A})}{\partial P_{ij}}. \quad (1)$$

Here η denotes the learning rate, which determines the step size taken in the parameter space at each iteration.

A key advantage of this framework is its seamless compatibility with modern machine learning infrastructure. Instead of the basic gradient descent update in Eq. (1), one may employ advanced optimizers such as *Adam*, incorporate learning-rate schedules, execute computations on GPUs, and monitor training dynamics in real time using *TensorBoard*. This integration allows network optimization problems to directly leverage the efficiency and robustness of contemporary differentiable programming tools.

Depending on the problem type, the parameters P_{ij} may be initialized randomly, uniformly, or using a mixture of both. The choice of initialization can significantly affect optimization stability and convergence behavior, and different problem classes may favor different strategies.

We further stabilize the optimization process by observing that, when a budget constraint is enforced, the free parameters \mathbf{P} may be rescaled without altering the encoded adjacency

matrix A . Although this scaling invariance leaves the forward map $\mathbf{A} = g(\mathbf{P})$ unchanged, it does influence gradient magnitudes and therefore affects optimization dynamics. Empirically, we find that stability improves when \mathbf{P} is renormalized after each gradient step to satisfy

$$\|\mathbf{P}\|_2 = \sqrt{E},$$

where E denotes the number of unmasked (i.e., admissible) edges, corresponding to the effective number of degrees of freedom. This renormalization is enabled by default in *GradNet*, but may be disabled by the user if desired.

In problems where the loss landscape contains many local minima, it can be beneficial to introduce stochastic smoothing to reduce the likelihood of becoming trapped. In *GradNet*, this is implemented by injecting noise into the parameters \mathbf{P} , thereby producing perturbed adjacency matrices \mathbf{A} in a neighborhood of the current iterate. A batch of such perturbations is sampled, the loss is evaluated at each sample, and the gradient is computed with respect to the averaged objective. This procedure acts as a local smoothing of the loss landscape and can substantially improve robustness. We explore this strategy further in Sec. IV-F.

IV. APPLICATIONS AND CASE STUDIES

A. Recurrent network for logical gates

We begin with a toy example, closely aligned with standard neural network training. We train small recurrent networks with adjacency matrix A_{ij} to implement the logical operations AND, OR, and XOR. Nodes $\{A, B\}$ serve as inputs and the output is written to node O .

The system state x_i is initialized with input values $\{x_A, x_B\}$, while all other nodes $i \notin \{A, B\}$ are set to zero. Computation consists of two iterations of the nonlinear update

$$\mathbf{x}(t+1) = \tanh(\mathbf{A}\mathbf{x}(t)).$$

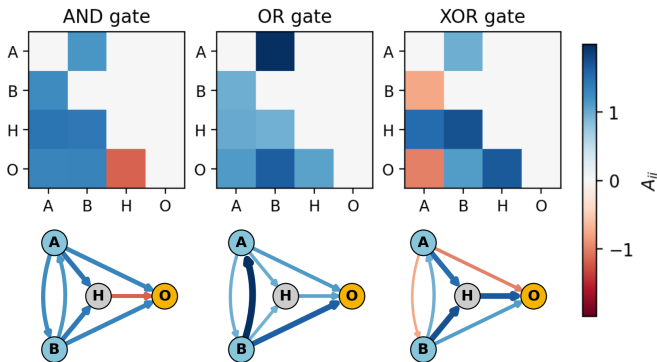


Fig. 2: **Networks that compute AND, OR, and XOR logical operations.** Nodes A and B serve as inputs, and after two iterations $\mathbf{x}(t+1) = \tanh(\mathbf{A}\mathbf{x}(t))$ the result is written to node O . H denotes a hidden node. The top row shows the optimized adjacency matrices, and the bottom row the corresponding network diagrams.

From a network-science perspective, this is message passing on a weighted directed graph. From a machine-learning perspective, it is equivalent to two bias-free linear layers with tanh activation. After two rounds, the output x_O encodes the logical result.

For each gate, we train a separate network using *GradNet*. The adjacency matrix A_{ij} is initialized randomly. For all four possible two-bit inputs $\{00, 01, 10, 11\}$, we compute the predicted outputs and define the loss as the ℓ_2 distance to the target truth table. The optimized networks are shown in Fig. 2. In all cases, the outputs round to the correct logical values.

Increasing the number of hidden nodes or allowing additional message-passing rounds improves accuracy and reduces the need for rounding. Notably, although all edges are admissible, the learned optimal networks are sparse. Because the dynamics is restricted to two iterations, information can propagate only along paths of length two; accordingly, the optimal architecture contains precisely those edges that participate in length-two paths from the input set $\{A, B\}$ to the output node O .

B. Structural Optimization: Algebraic connectivity

Our first example will optimize one of the most important global measures of networks, its algebraic connectivity [49], [50], i.e., the second Laplacian eigenvalue λ_2 . The Laplacian matrix of a network L_{ij} is defined in terms of the adjacency matrix as $L_{ij} = \delta_{ij} \sum_k A_{ik} - A_{ij}$. Its first eigenvalue λ_1 is always zero, provided that the $A_{ij} \geq 0$. The second eigenvalue λ_2 is a quantitative measure of connectivity and robustness. For example, it governs how fast diffusion converges on it, reveals natural partitions in its structure, and indicates how “tightly” the network is held together, hence improving it has been a target of interest [36], [51], [52].

We look for the best network with the constrained coupling budget

$$b = \frac{1}{N} \sum_{ij} A_{ij}. \quad (2)$$

It turns out that in general, optimal resource allocation with this goal produces a completely and uniformly connected graph. Hence, as a more interesting demonstration, we restrict the network to a 2D square lattice. This restriction is achieved simply by passing the adjacency matrix of the unweighted lattice network to the *GradNet* object as the “mask” argument. The results of this optimization are presented in Fig. 3.

Results indicate that, on a grid, edges near the center play a critical role and should be prioritized with more resources to enhance algebraic connectivity. Furthermore, it turns out that the weights of vertical edges are independent of their horizontal position, and horizontal ones are independent of the vertical positions.

The eigensystems for arbitrary network Laplacians are not analytically solvable in general. This remains true for square lattices with arbitrary edge weights. But, as discussed above, the optimality is a significant simplifying condition allowing much deeper analysis. We will demonstrate this below by deriving a closed-form expression for the optimal edge-weights maximizing λ_2 .

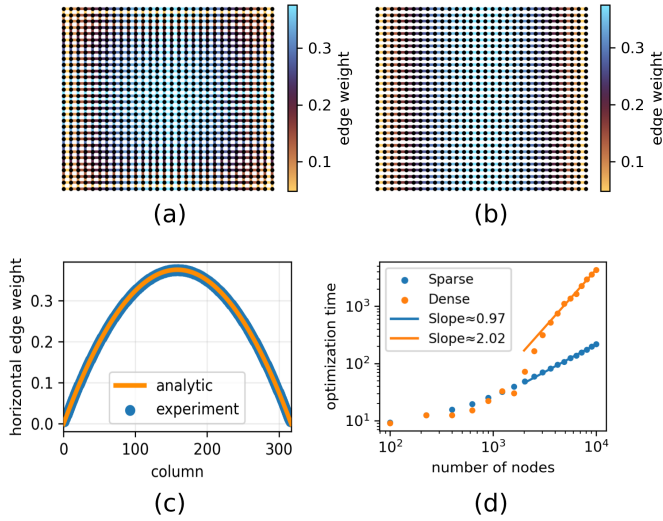


Fig. 3: Optimal square lattice maximizing the algebraic connectivity, i.e., the second Laplacian eigenvalue λ_2 , under the constrained budget in Eq. (2). (a) Heatmap of the optimal edge weights for a weighted 30×30 square lattice. (b) Horizontal edge weights plotted separately, revealing that they depend only on horizontal position (an analogous statement holds for vertical edges). (c) Comparison between the analytical optimum (Eq. (8)) in orange and the numerical optimum for 317×317 network, i.e., $N \approx 10^5$ nodes, optimized on an NVIDIA L40S GPU for 2.7 hours. (d) Optimization time (seconds) versus number of nodes N for a fixed number of optimization steps (50), comparing sparse and dense encodings on a MacBook with an M2 chip. Linear fits to the final eight data points indicate $O(N)$ scaling for the sparse encoding and $O(N^2)$ scaling for the dense encoding.

Let us first express the Laplacian matrix for the $n \times n$ square lattice. The nodes are indexed by i and j to indicate the vertical and horizontal positions respectively. We denote the horizontal edge weight connecting to the node (i, j) from right as a_{ij} . Similarly, the vertical edge weight connecting from below is denoted b_{ij} . Since we use two indices per node, the state vector x_{ij} also has two indices. In these terms, the action of the Laplacian operator $L_{ij;\alpha\beta}$ on the state x_{ij} can be expressed as

$$\begin{aligned}
 (\mathbf{L}\mathbf{x})_{ij} &= \sum_{\alpha\beta} L_{ij;\alpha\beta} x_{\alpha\beta} \\
 &= a_{i,j-1}(x_{ij} - x_{i,j-1}) + a_{ij}(x_{ij} - x_{i,j+1}) \\
 &\quad + b_{i-1,j}(x_{ij} - x_{i-1,j}) + b_{ij}(x_{ij} - x_{i+1,j})
 \end{aligned} \tag{3}$$

The first eigenvector of the Laplacian for a connected network is uniform $\mathbf{x}^{(1)} = \mathbf{1}$. With this, we can write down the variational characterization of the second eigenvalue

$$\begin{aligned}
 \lambda_2 &= \min_{\substack{\|\mathbf{x}\|=1 \\ \mathbf{x} \perp \mathbf{1}}} \mathbf{x}^\top \mathbf{L} \mathbf{x} \\
 &= \min_{\substack{\|\mathbf{x}\|=1 \\ \mathbf{x} \perp \mathbf{1}}} \sum_{ij} (a_{ij}(x_{ij} - x_{i,j+1})^2 + b_{ij}(x_{ij} - x_{i+1,j})^2).
 \end{aligned} \tag{4}$$

Here, the result on the second line is obtained by using Eq. (3) and simple algebraic transformations. Given the budget constraint Eq. (2), the structure is maximizing when the marginal gains of the performance target with respect to each of the edge weights is equal:

$$\begin{aligned}
 \frac{\partial \lambda_2}{\partial a_{ij}} &= \frac{\partial \lambda_2}{\partial b_{ij}} = \text{const. (independent of } i \text{ and } j) \\
 &= \left(x_{i+1,j}^{(2)} - x_{ij}^{(2)} \right)^2 = \left(x_{i,j+1}^{(2)} - x_{ij}^{(2)} \right)^2.
 \end{aligned} \tag{5}$$

Here $\mathbf{x}^{(2)}$ is the minimizer of Eq. (4), i.e., the second eigenvector. Using these conditions alongside with the condition $\mathbf{x} \perp \mathbf{1}$ we find two solutions for the second eigenvector, indicating that the second eigenvalue is degenerate

$$x_{ij}^{(2)} \propto i - j \quad \text{and} \quad x_{ij}^{(2)} \propto i + j - n - 1. \tag{6}$$

Recall that n here is the lattice length. Both of these eigenvectors must satisfy $\mathbf{L}\mathbf{x} = \lambda_2\mathbf{x}$. Using this with Eqs. (3) and (5) we get the two following conditions

$$\begin{aligned}
 \lambda_2(i - j) &= b_{i-1,j} - b_{ij} - a_{i,j-1} + a_{ij} \\
 \lambda_2(i + j - n - 1) &= b_{i-1,j} - b_{ij} + a_{i,j-1} - a_{ij}
 \end{aligned} \tag{7}$$

Solving this system of equations gives us $a_{ik} = b_{kj} = \frac{\lambda_2}{2} k(n - k)$. This captures the numerically observed property that vertical/horizontal edge weights only depend on the second/first index. Last missing piece, λ_2 , can be obtained by applying the normalization condition Eq. (2), resulting in $\lambda_2 = \frac{3b}{(n-1)(n+1)}$, giving us the closed-form expression for the optimal edge weights

$$a_{ik} = b_{kj} = \frac{3}{2} \frac{b}{(n-1)(n+1)} k(n-k). \tag{8}$$

This expression exhibits close agreement with numerical optimization results, as demonstrated in Fig. 3.

Optimizing algebraic connectivity on a grid also serves as an ideal scenario to explore advantages and disadvantages of sparse vs dense network encodings. On one hand, switching to sparse network encoding results in significant speed and memory boost, since we move from having to store and move $O(N^2)$ elements to $O(N)$ elements, where $N = n^2$ is the number of nodes. On the other hand, as soon as we drop the dense representations of the adjacency and Laplacian matrices, we can no longer perform operations that depend on the dense encoding, such as matrix inversion, diagonalization, and standard spectrum computation. Instead we have to resort to numerical methods.

For a sparsely encoded network, we compute λ_2 using a modified power method. Since the standard power method returns the eigenvalue of largest magnitude, whereas λ_2 is the

second-smallest Laplacian eigenvalue, we instead consider the shifted matrix

$$\tilde{L}_{ij} = c\delta_{ij} - L_{ij}. \quad (9)$$

Its eigenvalues satisfy $\tilde{\lambda}_i = c - \lambda_{N-i}$. By Gershgorin's circle theorem [53], the Laplacian eigenvalues are bounded above by $2 \max_i L_{ii}$; choosing $c = 2 \max_i L_{ii}$ ensures $\tilde{\lambda}_i \geq 0$, so they are ordered by magnitude.

The largest eigenvector of \tilde{L} corresponds to the constant eigenvector $\mathbf{v}_1 = \mathbf{1}/(\mathbf{1}^\top \mathbf{1})$ of L . We therefore initialize with a random vector \mathbf{r} and project out this component,

$$\mathbf{x}^{(0)} = \mathbf{r} - (\mathbf{r}^\top \mathbf{v}_1) \mathbf{v}_1, \quad (10)$$

and iterate

$$\mathbf{x}^{(k+1)} = \tilde{L} \mathbf{x}^{(k)}. \quad (11)$$

This converges to $\tilde{\mathbf{v}}_{N-1} = \mathbf{v}_2$, from which we compute λ_2 via the Rayleigh quotient,

$$\lambda_2 = \frac{\mathbf{v}_2^\top L \mathbf{v}_2}{\mathbf{v}_2^\top \mathbf{v}_2}. \quad (12)$$

The procedure relies only on matrix–vector multiplications, which are efficient for sparse matrices. Differentiating only through the Rayleigh quotient in Eq. (12) enables efficient optimization of edge weights. As shown in Fig. 3(d), the optimization time scales as $O(N)$ for sparse encoding and $O(N^2)$ for dense encoding, demonstrating the huge advantage of sparse encoding, whenever it is applicable.

C. Synchrony-Optimal Networks: Kuramoto Model

We now demonstrate how gradient-based network optimization can reveal structural principles governing nonlinear Kuramoto dynamics on networks [54]. This subsection reproduces the results reported in [29]. Rather than treating network topology as fixed and tuning a global coupling parameter, as is established in studies of synchronization [55], [5], we instead optimize the network itself under an explicit resource constraint. This perspective aligns with the extensive line of research on optimizing networks for synchrony [24], [25], [26], [27], [44], [28], while giving rise to novel network structures and fundamentally altered dynamics.

We focus on the Kuramoto model of heterogeneous phase oscillators,

$$\frac{d\theta_i}{dt} = \omega_i + \sum_{j=1}^N A_{ij} \sin(\theta_j - \theta_i), \quad (13)$$

where each node has an intrinsic frequency ω_i and interacts through a weighted, undirected network encoded by the adjacency matrix $A_{ij} \geq 0$. Rather than scaling all couplings uniformly, we impose a fixed total coupling budget

$$b = \frac{1}{N} \sum_{ij} A_{ij}, \quad (14)$$

and seek the network that maximizes collective synchrony subject to this constraint.

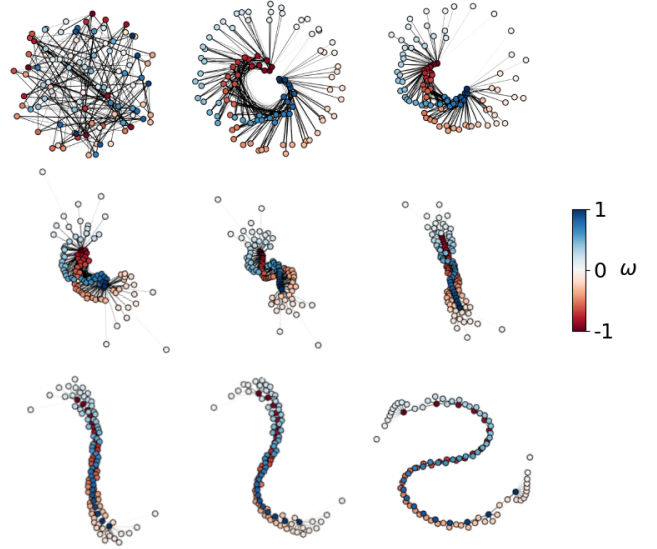


Fig. 4: Sequence of snapshots of evolving network to optimize synchronization. The node colors indicate intrinsic frequencies ω_i . Each subsequent snapshot supports higher value of synchronization order parameter. With this progress, the network becomes more and more sparse, bipartite (connections exist exclusively between red and blue nodes), monophilic (each node connects to a narrow range of neighboring frequencies, e.g., dark red connects to light blue nodes), and elongated (characterized by long path lengths).

This problem was studied in depth in our prior work [29], which serves as a canonical example of the *GradNet* framework in action. There, the optimization objective was defined as the long-time average of the Kuramoto order parameter,

$$r(t) = \left| \frac{1}{N} \sum_{j=1}^N e^{i\theta_j(t)} \right|, \quad (15)$$

and gradients were computed end-to-end through numerical integration of the dynamics using *GradNet*. Notice that each step in the gradient descent requires a new computation of the loss function and therefore a separate full integration of the dynamics.

Despite the apparent simplicity of the objective, gradient-based optimization consistently converges to highly nontrivial network structures. The optimal networks are:

- **Sparse**, with most potential edges eliminated despite no explicit sparsity penalty;
- **Bipartite**, connecting oscillators with frequencies of opposite sign;
- **Elongated**, exhibiting large diameters and long path lengths rather than small-world structure;
- **Extremely monophilic**, meaning that the neighbors of any node have very similar frequencies to one another while differing strongly from the node itself.

None of these features were imposed a priori. Instead, they emerge purely from optimization under constraints. These findings overturn several long-standing intuitions, most notably that dense, homogeneous, or short-path networks are optimal for synchronization, and demonstrate how constrained optimization can surface unexpected design principles that are difficult to anticipate analytically [56], [57], [58].

The emergent topology has profound dynamical implications. Optimized networks eliminate the classical synchronization threshold: partial synchrony exists for arbitrarily small budgets, and global phase-locking emerges sharply once the budget exceeds a calculable critical value. Moreover, the transition exhibits universal critical scaling distinct from that observed in fixed-topology networks.

Crucially, the numerical results obtained via *GradNet* were not merely empirical. The Kuramoto model on arbitrary weighted networks is not analytically solvable in general, and even coarse characterizations of its stationary states and phase transitions typically require numerical simulation. When the network is optimized for synchrony, however, the emergent structure induces strong regularities that admit a reduced, continuum description in the thermodynamic limit [29].

Using variational analysis, asymptotic methods, and symmetry constraints, this reduced formulation enables efficient numerical evaluation of the order parameter for arbitrary frequency distributions and yields closed-form results in important regimes, including near the phase-locking transition and in the strong-coupling limit. More broadly, this demonstrates a key principle of optimal network science: optimization can induce structural regularities that convert otherwise intractable network dynamics into mathematically structured and partially solvable problems, with theory and computation informing one another.

D. Empirical Network Enhancement: Zachary’s Karate Club

No network science toolkit would be complete without a demonstration of its performance on the canonical benchmark of Zachary’s Karate Club [59], [60]. It is a classic social network of 34 members whose friendships were recorded by Wayne Zachary in the 1970s. A conflict between the instructor and the club president eventually caused the club to split into two factions, making it a standard example for community detection.

In this example, we take an opinion dynamics view: the instructor and president hold fixed, opposing opinions that diffuse through the network. Friendships then rewire to reduce the social tension, favoring ties between members with similar opinions, which subsequently splits the graph into two components.

The opinion dynamics is given by a simple diffusion process

$$\dot{o}(t) = -L o(t). \quad (16)$$

Here L is the Laplacian matrix. The opinions of the president and the instructor are fixed $o_1(t) = 1$, $o_N(t) = -1$. Everyone else is initially indifferent $o_i(0) = 0$ for $1 < i < N$. The “social

tension” is measured by the weighted sum of disagreements between friends:

$$D(t) = \frac{\sum_{i,j} A_{ij} (o_i(t) - o_j(t))^2}{\sum_{i,j} A_{ij}}. \quad (17)$$

We initialize the *GradNet* optimization at the initial network Zachary measured, and optimize it from there. The final edges are restricted to be non-negative, and the allowed modifications are non-positive - to emulate breaking friendships. The loss function is defined as the long-time average of the social tension. Result of this optimization is shown in Fig. 5.

The edges represent the friendships after the social tension has been minimized. You can see that the network has split into two factions. The node colors, on the other hand, represent the ground truth: which club member sided with who. The network split produced by the opinion diffusion model matches the ground truth except for one member, a node that is widely known to be structurally ambiguous and is frequently misclassified by other community detection algorithms [61]. This example shows how clustering can emerge as a result of social pressure.

E. Network Reconstruction from Functional Observables

The examples discussed so far addressed network-scientific questions formulated and solved using gradient-based optimization. We now turn to a system identification example from the field of machine learning. Unlike the previous cases, this example begins with the introduction of data, which are used to train the model and infer the underlying network structure.

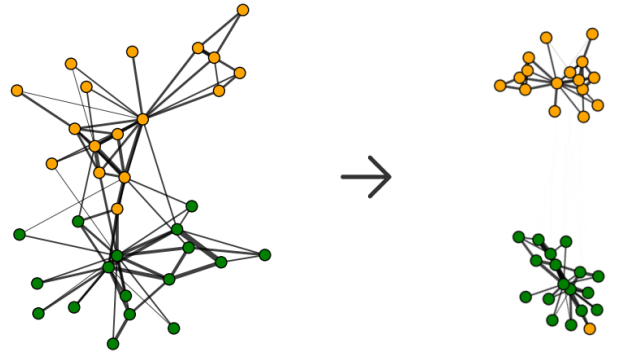


Fig. 5: **Opinion-dynamics-driven pruning of Zachary’s Karate Club network.** Left: Original friendship network of the 34-member *Zachary’s Karate Club*. Right: Optimized network obtained by minimizing the long-time average of the social tension Eq. (17) under the diffusion dynamics Eq. (16), with the instructor and president holding fixed opposing opinions. Edge weights can only decrease and are constrained to remain non-negative, modeling friendship removal. The optimized network splits into two connected components. Node colors indicate the ground-truth factions observed after the real split; the model recovers the empirical division with only one misclassified member.

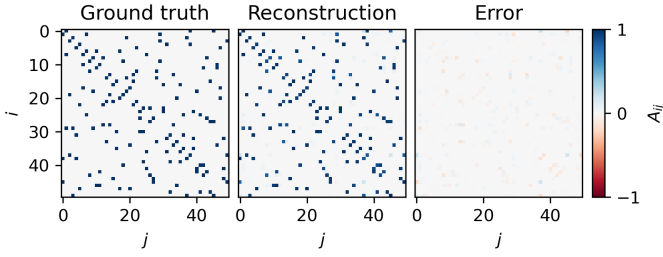


Fig. 6: **Optimization-based network reconstruction from oscillator phase trajectories.** (a) Ground-truth adjacency matrix of a random 3-regular network with $N = 50$ nodes used to generate Kuramoto phase trajectories $\{\theta^{(\tau)}\}$. (b) Adjacency matrix reconstructed by minimizing the prediction loss defined in Eq. (18). (c) Reconstruction error (well below 1); after binary thresholding, the recovered network exactly matches the ground truth.

Inferring the topology of interacting systems from observed dynamics is a long-standing problem in nonlinear dynamics and network science, with applications ranging from neuroscience to social and technological systems [62], [63], [64].

We simulate the Kuramoto model on a random 3-regular network of 50 nodes, and record the resulting phase trajectories $\theta^{(\tau)}$. These trajectories then serve as the data. Based on each state $\theta^{(\tau)}$, we predict the following state $\hat{\theta}^{(\tau+1)}$ after the time interval dt using numerical integration. The loss function then is defined as the prediction error

$$\mathcal{L}(\mathbf{A}) = \sum_{\tau, i} \left(\hat{\theta}_i^{(\tau)} - \theta_i^{(\tau)} \right)^2 \quad (18)$$

Minimizing this error naturally drives the network toward the ground-truth structure. We demonstrate this in Fig. 6 using a random 3-regular network with $N = 50$ nodes. *GradNet* learns both the correct connectivity pattern and the uniform edge weights directly from the observed phase data. Notably, sparsity is not explicitly enforced, but instead emerges naturally during the learning process.

F. Spatially Embedded Networks: Quantum Internet

Finally, we optimize the communication capacity of a quantum internet with lossy channels. Quantum networks aim to distribute entanglement and quantum information between spatially separated quantum processors, forming the backbone of future distributed quantum computing and secure communication infrastructures [65], [66]. The design of such networks involves nontrivial trade-offs between physical connectivity, channel losses, and resource constraints, and has therefore motivated a growing body of work on quantum network architecture and routing optimization [67], [68], [69].

The geographic placement of quantum computers are sampled randomly, and wiring costs are assumed to be proportional to the distance between nodes. We compute the pairwise distances D_{ij} , and optimize the adjacency matrix A_{ij} under the constrained construction budget.

$$b = \frac{1}{N} \sum_{ij} D_{ij} A_{ij}. \quad (19)$$

Following the derivations in [69], we define the transmissivity of each edge e as η_e . We model the edge transmissivities from the edge weights using the mapping $\eta_{ij} = \tanh A_{ij}$. The composite transmissivity along some path $P = \{e_1, e_2, \dots, e_K\}$ is given by the bottleneck transmissivity along the chain $\eta_P = \min_{e \in P} \eta_e$ (see [69] for details). And the capacity of this chain is given by

$$\mathcal{C}_P = -\log_2(1 - \eta_P). \quad (20)$$

The communication capacity between two nodes (i, j) in a network is the capacity of the best path P_{ij} connecting them

$$\mathcal{C}_{ij} = \max_{P_{ij}} \mathcal{C}_P = -\log_2(1 - \max_{P_{ij}} \min_{e \in P} \eta_e). \quad (21)$$

The mean network capacity, and the target of our optimization, is then given by

$$\mathcal{C} = \frac{1}{n(n-1)} \sum_{i \neq j} \mathcal{C}_{ij} = -\frac{1}{n(n-1)} \sum_{i \neq j} \log_2(1 - \max_{P_{ij}} \min_{e \in P} \eta_e). \quad (22)$$

Because the objective combines nested min and max operations, its loss landscape is highly non-smooth and can

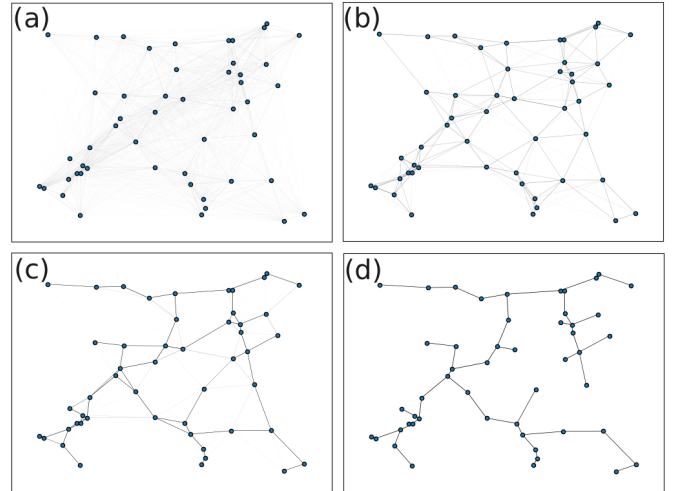


Fig. 7: **Optimization of a spatial quantum network converges to the minimum spanning tree.** Four snapshots of the weighted network A_{ij} during maximization of the mean communication capacity \mathcal{C} (Eq. (22)) under the geographic budget constraint (Eq. (19)), with edge costs proportional to inter-node distance. Starting from a dense initialization, stochastic smoothing (noise and batching) enables gradient descent to prune redundant links and reallocate weight to relieve bottlenecks implied by the nested min-max objective. The network progressively sparsifies while maintaining connectivity, and the final configuration matches the minimum spanning tree.

contain numerous shallow local minima that trap standard gradient-based optimization. To mitigate this, we introduce two additional hyperparameters, *noise* and *batch size*, and optimize a locally averaged objective. Rather than evaluating the objective once per update at \mathbf{P} , we draw a batch of b perturbed parameter vectors $\{\mathbf{P}_i\}_{i=1}^b$ in a neighborhood of \mathbf{P} such that $\|\mathbf{P} - \mathbf{P}_i\|_\infty \leq \epsilon$, where b denotes the batch size and ϵ the noise radius. We evaluate the objective at each \mathbf{P}_i , average these values, and then compute the gradient of this averaged objective to update \mathbf{P} via gradient descent. This procedure acts as a stochastic local smoothing (mollification) of the objective. With appropriate choices of b and ϵ , this can substantially suppress spurious local minima and improve optimization robustness.

Optimizing the quantum communication capacity in Eq. (22) subject to the geographically motivated budget constraint in Eq. (19), using the noise-and-batching procedure described above, recovers the minimum spanning tree as the optimal network architecture (Fig. 7). This outcome is intuitive: each node pair (i, j) contributes to the mean network capacity in Eq. (22) through its end-to-end bottleneck, since the nested min-max structure selects the weakest edge along the strongest available path. Consequently, the optimization induces a “bottleneck equalization” pressure that tends to level the effective edge weights along a chosen route and, by extension, across the network. Under a fixed budget, redundant alternative routes do not improve the objective, a spanning tree already provides a unique path between every pair, so the optimal resource allocation concentrates on maintaining connectivity while minimizing total cost. The resulting optimum is therefore the minimum spanning tree.

V. DISCUSSION

Studies of structural and dynamical properties of networks are usually performed on either fixed networks such as empirical networks or lattices, or on networks with fixed properties such as families of synthetic networks generated using algorithms. Much more rarely studies focus on optimized networks that arise through rewiring networks, mostly using MCMC, and even then some structural properties are baked into this search. Chief among such pre-determined properties is sparsity, an extremely prevalent property of real world networks, which has been routinely baked into network models as a fundamental property. Furthermore, most real networks are weighted, but very often they are analyzed as unweighted combinatorial graphs since the presence/absence of an edge is often deemed as the most important property of an edge. This perspective has unlocked tools from combinatorial graph theory and has helped reduce the complexity of the objects under study to enable elegant and insightful network scientific analysis.

In this paper, we argued for the usefulness of an additional alternative perspective: Rather than studying the structural properties of networks under a restrictive lens, we propose to consider all feasible weighted and potentially dense networks, and anchor the analysis on the purpose of the networked

system within the context of the hard design constraints like the construction budget and physical impossibility of some edges. This then reformulates the network scientific questions about the structure in terms of the constrained optimization of network fitness for the given purpose. This perspective unlocks new mathematical and computational tools like variational analysis, and gradient-based optimization, which naturally live and operate in the lifted space of weighted and potentially dense networks. We discussed the numerical gradient-based optimization tool designed for this purpose, discuss constructive mathematical models for such optimal structures, and discuss the emergent properties of such networks in different scenarios, such as emergent sparsity, bipartition, and community generation.

Such a variational or optimization-based perspective has proven remarkably fruitful across the sciences. In physics, for example, principles of least action or minimum energy underpin much of fundamental theory, from classical mechanics to General Relativity and Quantum Field Theory. In statistical mechanics, free energy minimization and entropy maximization provide a unifying framework for equilibrium and near-equilibrium phenomena. More recently, hand-crafted, rule-based systems have been largely supplanted by loss minimization in machine learning, where complex behavior emerges from the optimization of simple objectives. Across these domains, optimization principles serve not merely as computational tools, but as organizing concepts (see Table I).

These case studies highlight the broader promise of gradient-based network optimization. By allowing topology and weights to adapt continuously under explicit constraints, one can uncover emergent architectures, dynamical regimes, and scaling laws that remain inaccessible to traditional heuristic or combinatorial approaches. Importantly, these methods do not replace theory; instead, they act as a systematic probe of high-dimensional design spaces, revealing structure that can later be distilled into analytical insight.

These examples thus serve as a paradigmatic demonstration of *GradNet*'s role within optimal network science: optimization is not only a tool for engineering better networks, but also a mechanism for discovering new and analytically tractable structure-function relationships in complex systems.

REFERENCES

- [1] R. Albert and A.-L. Barabási, “Statistical mechanics of complex networks,” *Reviews of modern physics*, vol. 74, no. 1, p. 47, 2002.
- [2] M. Newman, *Networks*. Oxford university press, 2018.
- [3] M. E. Newman, “The structure and function of complex networks,” *SIAM review*, vol. 45, no. 2, pp. 167–256, 2003.
- [4] S. Boccaletti, V. Latora, Y. Moreno, M. Chavez, and D.-U. Hwang, “Complex networks: Structure and dynamics,” *Physics reports*, vol. 424, no. 4-5, pp. 175–308, 2006.
- [5] A. Arenas, A. Díaz-Guilera, J. Kurths, Y. Moreno, and C. Zhou, “Synchronization in complex networks,” *Physics reports*, vol. 469, no. 3, pp. 93–153, 2008.
- [6] A. Barrat, M. Barthelemy, and A. Vespignani, *Dynamical processes on complex networks*. Cambridge university press, 2008.
- [7] R. Pastor-Satorras, C. Castellano, P. Van Mieghem, and A. Vespignani, “Epidemic processes in complex networks,” *Reviews of modern physics*, vol. 87, no. 3, pp. 925–979, 2015.

- [8] P. Erdős and A. Rényi, "On random graphs i," *Publicationes Mathematicae*, vol. 6, pp. 290–297, 1959.
- [9] D. J. Watts and S. H. Strogatz, "Collective dynamics of 'small-world' networks," *Nature*, vol. 393, no. 6684, pp. 440–442, 1998.
- [10] J. M. Carlson and J. Doyle, "Highly optimized tolerance: Robustness and design in complex systems," *Physical review letters*, vol. 84, no. 11, p. 2529, 2000.
- [11] J. R. Banavar, A. Maritan, and A. Rinaldo, "Size and form in efficient transportation networks," *Nature*, vol. 399, no. 6732, pp. 130–132, 1999.
- [12] M. Kaiser and C. C. Hilgetag, "Nonoptimal component placement, but short processing paths, due to long-distance projections in neural systems," *PLoS computational biology*, vol. 2, no. 7, p. e95, 2006.
- [13] F. Corson, "Fluctuations and redundancy in optimal transport networks," *Physical Review Letters*, vol. 104, no. 4, p. 048703, 2010.
- [14] R. F. I. Cancho and R. V. Solé, "Optimization in complex networks," in *Statistical mechanics of complex networks*. Springer, 2003, pp. 114–126.
- [15] M. Buchanan, "The best is yet to come," *Nature*, vol. 447, no. 7140, pp. 39–39, 2007.
- [16] L. F. Seoane and R. Solé, "Phase transitions in pareto optimal complex networks," *Physical Review E*, vol. 92, no. 3, p. 032807, 2015.
- [17] C. M. Schneider, A. A. Moreira, J. S. Andrade Jr, S. Havlin, and H. J. Herrmann, "Mitigation of malicious attacks on networks," *Proceedings of the National Academy of Sciences*, vol. 108, no. 10, pp. 3838–3841, 2011.
- [18] H. J. Herrmann, C. M. Schneider, A. A. Moreira, J. S. Andrade Jr, and S. Havlin, "Onion-like network topology enhances robustness against malicious attacks," *Journal of Statistical Mechanics: Theory and Experiment*, vol. 2011, no. 01, p. P01027, 2011.
- [19] A. Zeng and W. Liu, "Enhancing network robustness against malicious attacks," *Physical Review E—Statistical, Nonlinear, and Soft Matter Physics*, vol. 85, no. 6, p. 066130, 2012.
- [20] V. H. Louzada, F. Daolio, H. J. Herrmann, and M. Tomassini, "Smart rewiring for network robustness," *Journal of Complex networks*, vol. 1, no. 2, pp. 150–159, 2013.
- [21] Y. Yang, Z. Li, Y. Chen, X. Zhang, and S. Wang, "Improving the robustness of complex networks with preserving community structure," *PLoS one*, vol. 10, no. 2, p. e0116551, 2015.
- [22] H. Chan and L. Akoglu, "Optimizing network robustness by edge rewiring: a general framework," *Data Mining and Knowledge Discovery*, vol. 30, no. 5, pp. 1395–1425, 2016.
- [23] S. Massei and F. Tudisco, "Optimizing network robustness via krylov subspaces," *ESAIM: Mathematical Modelling and Numerical Analysis*, vol. 58, no. 1, pp. 131–155, 2024.
- [24] A. E. Motter, C. Zhou, and J. Kurths, "Network synchronization, diffusion, and the paradox of heterogeneity," *Physical Review E—Statistical, Nonlinear, and Soft Matter Physics*, vol. 71, no. 1, p. 016116, 2005.
- [25] L. Donetti, P. I. Hurtado, and M. A. Munoz, "Entangled networks, synchronization, and optimal network topology," *Physical Review Letters*, vol. 95, no. 18, p. 188701, 2005.
- [26] A. A. Rad, M. Jalili, and M. Hasler, "Efficient rewirings for enhancing synchronizability of dynamical networks," *Chaos: An Interdisciplinary Journal of Nonlinear Science*, vol. 18, no. 3, 2008.
- [27] T. E. Gorochoowski, M. di Bernardo, and C. S. Grierson, "Evolving enhanced topologies for the synchronization of dynamical complex networks," *Physical Review E—Statistical, Nonlinear, and Soft Matter Physics*, vol. 81, no. 5, p. 056212, 2010.
- [28] D. Taylor, P. S. Skardal, and J. Sun, "Synchronization of heterogeneous oscillators under network modifications: Perturbation and optimization of the synchrony alignment function," *SIAM journal on applied mathematics*, vol. 76, no. 5, pp. 1984–2008, 2016.
- [29] G. Mikaberidze and D. Taylor, "Emergent topology of optimal networks for synchrony," *arXiv preprint arXiv:2509.18279*, 2025.
- [30] S. Boyd, P. Diaconis, and L. Xiao, "Fastest mixing markov chain on a graph," *SIAM review*, vol. 46, no. 4, pp. 667–689, 2004.
- [31] S. Saha, A. Adiga, B. A. Prakash, and A. K. S. Vullikanti, "Approximation algorithms for reducing the spectral radius to control epidemic spread," in *Proceedings of the 2015 SIAM International Conference on Data Mining*. SIAM, 2015, pp. 568–576.
- [32] L. T. Le, T. Eliassi-Rad, and H. Tong, "Met: A fast algorithm for minimizing propagation in large graphs with small eigen-gaps," in *Proceedings of the 2015 SIAM International Conference on Data Mining*. SIAM, 2015, pp. 694–702.
- [33] D. Xue and S. Hirche, "Distributed topology manipulation to control epidemic spreading over networks," *IEEE Transactions on Signal Processing*, vol. 67, no. 5, pp. 1163–1174, 2018.
- [34] W.-X. Wang, X. Ni, Y.-C. Lai, and C. Grebogi, "Optimizing controllability of complex networks by minimum structural perturbations," *Physical Review E—Statistical, Nonlinear, and Soft Matter Physics*, vol. 85, no. 2, p. 026115, 2012.
- [35] C. O. Becker, S. Pequito, G. J. Pappas, and V. M. Preciado, "Network design for controllability metrics," *IEEE Transactions on Control of Network Systems*, vol. 7, no. 3, pp. 1404–1415, 2020.
- [36] A. Ghosh and S. Boyd, "Growing well-connected graphs," in *Proceedings of the 45th IEEE Conference on Decision and Control*. IEEE, 2006, pp. 6605–6611.
- [37] A. Ghosh, S. Boyd, and A. Saberi, "Minimizing effective resistance of a graph," *SIAM review*, vol. 50, no. 1, pp. 37–66, 2008.
- [38] S. Patwardhan, M. Barthelemy, Ş. Erkol, S. Fortunato, and F. Radicchi, "Symmetry breaking in optimal transport networks," *Nature Communications*, vol. 15, no. 1, p. 3758, 2024.
- [39] M. T. Gastner and M. E. Newman, "Optimal design of spatial distribution networks," *Physical Review E—Statistical, Nonlinear, and Soft Matter Physics*, vol. 74, no. 1, p. 016117, 2006.
- [40] L. M. Pecora and T. L. Carroll, "Master stability functions for synchronized coupled systems," *Physical review letters*, vol. 80, no. 10, p. 2109, 1998.
- [41] Y. Wang, D. Chakrabarti, C. Wang, and C. Faloutsos, "Epidemic spreading in real networks: An eigenvalue viewpoint," in *22nd international symposium on reliable distributed systems, 2003. proceedings*. IEEE, 2003, pp. 25–34.
- [42] L. Donetti, F. Neri, and M. A. Munoz, "Optimal network topologies: expanders, cages, ramanujan graphs, entangled networks and all that," *Journal of Statistical Mechanics: Theory and Experiment*, vol. 2006, no. 08, pp. P08007–P08007, 2006.
- [43] J. Wu, M. Barahona, Y.-J. Tan, and H.-Z. Deng, "Spectral measure of structural robustness in complex networks," *IEEE Transactions on Systems, Man, and Cybernetics-Part A: Systems and Humans*, vol. 41, no. 6, pp. 1244–1252, 2011.
- [44] P. S. Skardal, D. Taylor, and J. Sun, "Optimal synchronization of complex networks," *Physical review letters*, vol. 113, no. 14, p. 144101, 2014.
- [45] Z. Zhang, S. Lu, Z. Huang, and Z. Zhao, "Graph neural networks with adaptive structures," *IEEE Journal of Selected Topics in Signal Processing*, vol. 19, no. 1, pp. 181–194, 2024.
- [46] Y. Lu and Z. Lin, "Aro-gnn: Adaptive relation-optimized graph neural networks," *Journal of King Saud University Computer and Information Sciences*, vol. 37, no. 7, p. 174, 2025.
- [47] A. G. Baydin, B. A. Pearlmutter, A. A. Radul, and J. M. Siskind, "Automatic differentiation in machine learning: a survey," *Journal of machine learning research*, vol. 18, no. 153, pp. 1–43, 2018.
- [48] G. Mikaberidze, B. Mikaberidze, and D. Taylor, "Gradnet: A python package for optimal network science," <https://github.com/mikaberidze/gradnet>, 2026.
- [49] M. Fiedler, "Algebraic connectivity of graphs," *Czechoslovak mathematical journal*, vol. 23, no. 2, pp. 298–305, 1973.
- [50] N. M. M. De Abreu, "Old and new results on algebraic connectivity of graphs," *Linear algebra and its applications*, vol. 423, no. 1, pp. 53–73, 2007.
- [51] D. Mosk-Aoyama, "Maximum algebraic connectivity augmentation is np-hard," *Operations Research Letters*, vol. 36, no. 6, pp. 677–679, 2008.
- [52] N. Somisetty, H. Nagarajan, and S. Darbha, "Optimal robust network design: Formulations and algorithms for maximizing algebraic connectivity," *IEEE Transactions on Control of Network Systems*, vol. 12, no. 1, pp. 918–929, 2024.
- [53] S. A. Gershgorin, "Über die abgrenzung der eigenwerte einer matrix," *Izv. Akad. Nauk SSSR Ser. Mat.*, no. 6, pp. 749–754, 1931.
- [54] Y. Kuramoto, "International symposium on mathematical problems in theoretical physics," *Lecture Notes in Physics*, vol. 30, p. 420, 1975.
- [55] S. H. Strogatz, "From Kuramoto to Crawford: exploring the onset of synchronization in populations of coupled oscillators," *Physica D: Nonlinear Phenomena*, vol. 143, no. 1–4, pp. 1–20, 2000.
- [56] H. Hong, M.-Y. Choi, and B. J. Kim, "Synchronization on small-world networks," *Physical Review E*, vol. 65, no. 2, p. 026139, 2002.
- [57] T. Nishikawa, A. E. Motter, Y.-C. Lai, and F. C. Hoppensteadt, "Heterogeneity in oscillator networks: Are smaller worlds easier to synchronize?" *Physical Review Letters*, vol. 91, no. 1, p. 014101, 2003.

- [58] D. Kelly and G. A. Gottwald, "On the topology of synchrony optimized networks of a kuramoto-model with non-identical oscillators," *Chaos: An Interdisciplinary Journal of Nonlinear Science*, vol. 21, no. 2, 2011.
- [59] W. W. Zachary, "An information flow model for conflict and fission in small groups," *Journal of anthropological research*, vol. 33, no. 4, pp. 452–473, 1977.
- [60] S. Fortunato, "Community detection in graphs," *Physics reports*, vol. 486, no. 3-5, pp. 75–174, 2010.
- [61] M. E. Newman and M. Girvan, "Finding and evaluating community structure in networks," *Physical review E*, vol. 69, no. 2, p. 026113, 2004.
- [62] G. Tirabassi, R. Sevilla-Escoboza, J. M. Buldú, and C. Masoller, "Inferring the connectivity of coupled oscillators from time-series statistical similarity analysis," *Scientific reports*, vol. 5, no. 1, p. 10829, 2015.
- [63] A. Pikovsky, "Reconstruction of a random phase dynamics network from observations," *Physics Letters A*, vol. 382, no. 4, pp. 147–152, 2018.
- [64] T. Gaskin, G. A. Pavliotis, and M. Girolami, "Inferring networks from time series: A neural approach," *PNAS nexus*, vol. 3, no. 4, p. pgae063, 2024.
- [65] H. J. Kimble, "The quantum internet," *Nature*, vol. 453, no. 7198, pp. 1023–1030, 2008.
- [66] S. Wehner, D. Elkouss, and R. Hanson, "Quantum internet: A vision for the road ahead," *Science*, vol. 362, no. 6412, p. eaam9288, 2018.
- [67] R. Van Meter and S. J. Devitt, "The path to scalable distributed quantum computing," *Computer*, vol. 49, no. 9, pp. 31–42, 2016.
- [68] L. Gyongyosi and S. Imre, "Entanglement availability differentiation service for the quantum internet," *Scientific reports*, vol. 8, no. 1, p. 10620, 2018.
- [69] S. Pirandola, "End-to-end capacities of a quantum communication network," *Communications Physics*, vol. 2, no. 1, p. 51, 2019.